Quantum Monte Carlo studies of superfluid Fermi gases

S. Y. Chang and V. R. Pandharipande
Department of Physics, University of Illinois at Urbana-Champaign, 1110 West Green Street, Urbana, Illinois 61801, USA

J. Carlson
Theoretical Division, Los Alamos National Laboratory, Los Alamos, New Mexico 87545, USA

K. E. Schmidt
Department of Physics and Astronomy, Arizona State University, Tempe, Arizona 85287, USA
(Received 24 April 2004; published 5 October 2004)

We report results of quantum Monte Carlo calculations of the ground state of dilute Fermi gases with attractive short-range two-body interactions. The strength of the interaction is varied to study different pairing regimes which are characterized by the product of the *s*-wave scattering length and the Fermi wave vector, ak_F. We report results for the ground-state energy, the pairing gap Δ, and the quasiparticle spectrum. In the weak-coupling regime, $1/ak_F<-1$, we obtain Bardeen-Cooper-Schrieffer (BCS) superfluid and the energy gap Δ is much smaller than the Fermi gas energy E_{FG}. When $a>0$, the interaction is strong enough to form bound molecules with energy E_{mol}. For $1/ak_F \gtrsim 0.5$, we find that weakly interacting composite bosons are formed in the superfluid gas with Δ and gas energy per particle approaching $|E_{\mathrm{mol}}|/2$. In this region, we seem to have Bose-Einstein condensation (BEC) of molecules. The behavior of the energy and the gap in the BCS-to-BEC transition region, $-0.5<1/ak_F<0.5$, is discussed.

DOI: 10.1103/PhysRevA.70.043602 PACS number(s): 03.75.Ss, 05.30.Fk, 21.65.+f

I. INTRODUCTION

How pairing evolves from the bare interaction has been a major question in condensed-matter physics, and the study of pairing in relation to the phenomenon of superfluidity and superconductivity can be traced back to Cooper *et al.* [1]. Pairing lies at the core of several quantum many-body problems, and it is also believed to influence the evolution of neutron stars [2]. Here we report results of quantum Monte Carlo calculations of a superfluid Fermi gas with short-range two-body interactions. The strength of the interaction is varied to study different regimes of pairing.

The evolution of pairing with the strength of the interaction has been discussed in the literature [3,4]. In the regime where the interaction is weak and attractive, a gas of fermions has a superconducting instability at low temperatures, and a gas of Cooper pairs is formed. The typical coherence length is larger than the interparticle spacing r_0 ($4\pi r_0^3\rho=3$ with ρ the number density) and the bound pairs overlap. In contrast, in the strong-coupling limit the coherence length is small, and the bound pairs can be treated as well-separated Bose molecules. One then expects the molecules to undergo Bose-Einstein condensation (BEC) into a single quantum state with zero momentum.

The Bardeen-Cooper-Schrieffer (BCS) theory [3] and Gorkov equations [5] have been used to estimate gaps in superfluid gases. However, their predictions differ by more than a factor of 2 and they may be qualitatively valid only in the weakly interacting regime. Here we use first-principles quantum Monte Carlo methods to study the entire region ranging from free fermions to the tightly bound Bose molecules.

Dilute Fermi gases of ^{40}K, ^{6}Li, ^{2}H, for example, can now be studied in the laboratory using magnetic and optical trapping and ingenious cooling methods [6,7]. These are dilute Fermi systems, in contrast to dense atomic liquid ^{3}He or a solution of ^{3}He in superfluid ^{4}He. Within the past few years, temperatures $T \ll T_F$ have been achieved, where $T_F=\hbar^2k_F^2/2m$ is the Fermi kinetic energy and k_F is the Fermi wave vector. At such a low temperature, the fermionic nature of the quantum statistics becomes evident in the measurement of the density profile of the trapped gas. At even lower temperatures, the transition to the superfluid Cooper-paired state is expected. However, the temperature T_c of this transition can be much lower than T_F and conclusive evidence of superfluidity is still to be seen. In order to have the transition at an achievable temperature, the experimentalists rely on the Feshbach resonance technique to produce strong interaction between the fermionic atoms.

When the range of the interatomic interaction is smaller than all the length scales in the system, the details of the interaction are believed to be unnecessary and the scattering length a is sufficient to characterize it. Near the resonance, the magnitude of the scattering length a becomes much larger than r_0 and the system enters the strong-coupling regime. The value $ak_F \sim -7.4$ has been achieved by O'Hara *et al.* [7] and the limit ($ak_F \to -\infty$) is now approached in the laboratory [8,9]. Recently, creation of bosonic molecules from ^{40}K atoms was reported by Regal *et al.* [10], and pairing in the $1/ak_F \sim 0$ regime was observed (Ref. 11).

A few words are in order regarding the language of *s*-wave scattering. For a noninteracting system at zero temperature, the only length scale is $1/k_F$. We can use the dimensionless quantity ak_F to describe a dilute gas having interparticle spacing r_0 much greater than the interaction range. We often use $1/ak_F$ because ak_F changes discontinuously from $-\infty$ to $+\infty$ when a bound state is formed at $1/ak_F=0$. For attractive interactions $1/ak_F$ can change from large nega-

tive values (weakly interacting limit) to large positive values (strongly interacting limit). As discussed in Sec. II, the radius of the bound molecule provides another length scale in the strongly interacting regime. Some physical examples of the limits of $1/ak_F$ are (i) electrons in superconductors have $1/ak_F$ large and negative; (ii) neutron matter has $1/ak_F$ small and negative; and (iii) cold deuterium atoms have large positive $1/ak_F$. In the last case, molecular bound states smaller than the average interparticle distance r_0 are possible. On the other hand, superfluid ^{3}He is not describable in terms of ak_F, because the interaction range is greater than r_0, and the paired state does not have *s*-wave symmetry.

In the limit of zero energy for the colliding pair, the two-body scattering cross section σ is given by $4\pi a^2$. When $|a| \ll r_0$, the interatomic collisions in the gas are similar to those in vacuum, and the mean free path is approximately given by $\ell = 1/\sigma\rho$. However, this approximation is meaningful only when $|a| \ll r_0$ and $\ell > r_0$. When $|a|$ is $\gtrsim r_0$, the two-body collisions in the gas are strongly influenced by the presence of other particles, and their cross section in the gas is much smaller than in vacuum.

For a Fermi gas at low density, an expansion of the energy in terms of ak_F is possible. For spin-1/2 Fermi gases, it is known to be [12,13]

$$\frac{E}{N} = E_{\mathrm{FG}}\left[1 + \frac{10}{9\pi}(ak_F) + \frac{4}{21}(11 - 2\ln 2)(ak_F)^2 + O(ak_F)^3 + \cdots\right], \tag{1}$$

where $E_{\mathrm{FG}} = 3/5(\hbar^2 k_F^2/2m) = (3/5)T_F$ is the ground-state energy per particle of the noninteracting Fermi gas. In the $ak_F \to -\infty$ limit, theoretical estimates of 0.326 and 0.568 E_{FG} were reported [14,15]. More recently, the authors [16] predicted $E_0 = (0.44 \pm 0.01)E_{\mathrm{FG}}$ using quantum Monte Carlo methods. In this paper, we continue that study of the properties of cold dilute spin-1/2 fermion gas and extend it to all the regimes of $1/ak_F$ as a first step for understanding the superfluidity and the bosonization of dilute Fermi gases.

The model considered in this study consists of A fermions contained in a box with periodic conditions on its boundaries. It is not polarized so that half of the spins point up and the other half down. Typically A is varied from 10 to 20 to estimate properties of uniform gas in the $A \to \infty$ thermodynamic limit. In some cases, larger values of A are used. Fermions of the same spin do not feel the effects of interaction because it is of short range and Pauli exclusion predominates. The fermions of different spins interact via a central potential $v(r)$ with the following properties: (i) It is attractive with very short range as we assume the dilute limit, (ii) the details of the potential do not matter, in principle we can think of it as an attractive δ-function potential, and (iii) the potential can be adjusted such that we can sweep through different regimes of ak_F.

From the considerations mentioned above, a cosh potential of the form

$$v(r) = -v_0 \frac{2\hbar^2}{m}\frac{\mu^2}{\cosh^2(\mu r)}, \tag{2}$$

can be used. The strength of potential (v_0) is adjusted to obtain the desired value of ak_F. We can also take appropriate values of μ such that the effective range of the potential R_{eff} is much smaller than the interparticle distance r_0. When $v_0 = 1$ this potential has $a = \pm\infty$ and $R_{\mathrm{eff}} = 2/\mu$. In most calculations we have used $\mu r_0 = 12$. For the $a \to -\infty$ case we also tested the $\mu r_0 \to \infty$ limit using $\mu r_0 = 24$ [16].

Results of simple lowest-order constraint variational (LOCV) calculations are reported in Sec. II. The LOCV method was first used to study neutron matter [17]. Recently, Cowell *et al.* [18] have used it to study cold Bose gases in the unstable $a > r_0$ regime. It provides a surprisingly good estimate of the ground-state energy. Here we use it to study the effect of the difference between the $\cosh(\mu r_0 = 12)$ and δ-function potentials on the energy of dilute gases. The difference becomes significant when $1/ak_F \to \infty$, and the radius of the molecule approaches $1/\mu$. LOCV is also used to estimate the energy of the unstable state of the Fermi gas for $a > 0$. The stability of dilute gases is discussed in the LOCV Sec. II.

One of the limitations of LOCV is that it cannot be used to calculate the pairing energy gap Δ or the other superfluid properties of Fermi gases. The quantum Monte Carlo methods used in Ref. 16 and this work to study superfluid gases are described in Sec. III, and the results for the energy, pairing gap and the quasiparticle spectrum are presented in Sec. IV over the range $ak_F = -1$ to $\mp\infty$ to +0.5. Conclusions are given in Sec. V.

II. LOWEST-ORDER CONSTRAINT VARIATIONAL CALCULATIONS

In the lowest-order constraint variational (LOCV) method, the ground state of the Hamiltonian

$$\mathcal{H} = -\frac{\hbar^2}{2m}\sum_{p=1}^{A}\nabla_p^2 + \sum_{i,j'} v(r_{ij'}), \tag{3}$$

where the unprimed index i denotes spin-up particle, primed index j' denotes spin-down particle, and p can be any particle, is approximated by the Jastrow-Slater wave function

$$|\Psi_V\rangle = \prod_{i,j'} f(r_{ij'})|\Phi_S\rangle, \tag{4}$$

where $|\Phi_S\rangle$ is the ground state of noninteracting fermions. In the present case, $|\Phi_S\rangle$ is a product of two Slater determinants, the first corresponding to the spin-up fermions and the second corresponding to the spin-down fermions. The interaction effects are represented by the Jastrow function $\Pi_{i,j'} f(r_{ij'})$, where $f(r_{ij'})$ denotes the pair correlation function. We often use $f_{ij'}$ to denote $f(r_{ij'})$. $f_{ij'} = 1$ means no correlation between the pair ij' and $f_{ij'} \neq 1$ for correlated pairs. In variational calculations, the function $f(r)$ is determined by minimizing the expectation value of the Hamiltonian

$$\langle \mathcal{H} \rangle = \frac{-\frac{\hbar^2}{2m}\sum_p \langle \Phi_S | \prod_{\alpha,\beta'} f_{\alpha\beta'} \nabla_p^2 \prod_{\gamma,\mu'} f_{\gamma\mu'} | \Phi_S \rangle + \sum_{i,j'} \langle \Phi_S | \prod_{\alpha,\beta'} f_{\alpha\beta'} v_{ij'} \prod_{\gamma,\mu'} f_{\gamma\mu'} | \Phi_S \rangle}{\langle \Phi_S | \prod_{\alpha,\beta'} f_{\alpha\beta'} \prod_{\gamma,\mu'} f_{\gamma\mu'} | \Phi_S \rangle}. \tag{5}$$

The assumption behind LOCV is that the energy is most sensitive to the correlations of short (less than r_0) range. We impose a constraint on the range of $f(r)$ to assure that the correlations are mostly among the closest pairs, and keep only the pair terms in the cluster expansion of the energy expectation value. The healing distance d is the range of $f(r)$ defined such that $f(r>d)=1$ and $df(r)/dr|_{r=d}=0$. In LOCV, d is chosen such that on average there is only one other particle within the distance d of any particle. Effects of deviations from this average are assumed to cancel.

Euler-Lagrange minimization of the energy expectation value [19] gives a Schrödinger-like equation for $f(r<d)$,

$$-\frac{\hbar^2}{m}\nabla^2 f(r) + v(r) f(r) = \lambda f(r). \tag{6}$$

The constraint used to determine the healing distance is

$$\frac{\rho}{2}\int_0^d f^2(r) d^3\mathbf{r} = 1, \tag{7}$$

and the λ is chosen such that $df(r)/dr|_{r=d}=0$. In Eqs. (6) and (7) we do not have exchange contributions because the range of the interaction is short and fermions of the same spin do not interact. When Eqs. (6) and (7) are simultaneously solved, the energy per particle is given by

$$E_{\mathrm{LOCV}} = E_{\mathrm{FG}} + \frac{\lambda}{2}. \tag{8}$$

The results obtained for the ground-state energy of spin-1/2 Fermi gas with the cosh and δ-function potentials are shown in Fig. 1.

When $1/ak_F<0$, the r_0 is the only length scale in the gas, and the results obtained with the cosh potential with $\mu r_0=12$ are indistinguishable from those given by the δ-function potential. In contrast, when $1/ak_F>0$, we have a molecular bound state whose radius provides another length scale. At large positive values of $1/ak_F$ there are differences between results of the present cosh and δ-function potentials due to the rms radius, R_{rms} of the molecule becoming comparable to the range of the present cosh potential. For example, at $1/ak_F=2$ we get $\mu R_{\mathrm{rms}}=2.3$ with the present choice of μ. In principle, we can continue to approximate the δ-function interaction with the cosh potential by further increasing μ, and working in the $\mu R_{\mathrm{rms}}\to\infty$ limit. However, all of the present computations are with $\mu r_0=12$.

Figure 1 also shows the presumably exact results obtained with the cosh potential with the Green's-function Monte Carlo (GFMC) method described in the next section. The LOCV energies appear to be surprisingly accurate. However, it should be realized that a part of the accuracy of LOCV is due to a cancellation of errors, and not due to the quality of the Jastrow-Slater variational wave function [Eq. (4)]. In fact, the variational energy upper bound obtained with that wave function for $1/ak_F=0$ is $=(0.62\pm0.01)E_{\mathrm{FG}}$, significantly above the GFMC result of $(0.44\pm0.01)E_{\mathrm{FG}}$. The LOCV energy of $0.46E_{\mathrm{FG}}$ is below the Jastrow-Slater variational upper bound because it is calculated approximately keeping only two-body cluster contributions. However, when the contributions of $\geqslant$ three-body clusters become important, we can expect that the approximations in the Jastrow-Slater wave function would also become important, and the true energy will be below the Jastrow-Slater upper bound.

The ground-state energies obtained with the conventional BCS (variational) method are also shown in Fig. 1. In the weakly interacting limit, $1/ak_F\to-\infty$, the BCS energy is too large since it does not have the correct low-density limit given by Eq. (1). On the other hand, in the strongly interacting limit, $1/ak_F\to+\infty$, the BCS energy is very close to the exact result (GFMC) presumably because in this limit we have complete pairing of the fermions into Bose molecules. LOCV is less accurate than the conventional BCS method in the strong-coupling region.

The LOCV pair correlation functions are shown in Fig. 2. The healing distance $d\approx r_0$ in the weakly interacting region $(1/ak_F\ll 0)$, and as we increase the strength of the potential, $f(r)$ becomes more and more peaked at the origin, and d becomes smaller than r_0. In fact for $1/ak_F\gg 0$, the boundary condition at d has less impact on E_{LOCV} and λ of Eq. (6)

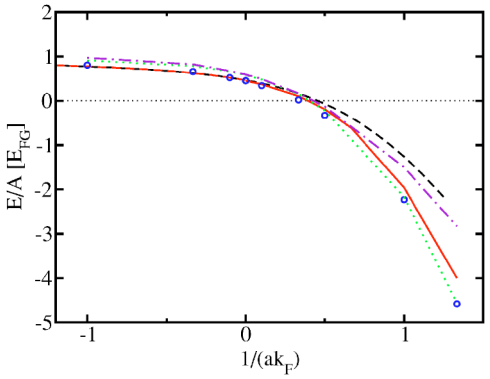

FIG. 1. Ground-state energy per particle of dilute Fermi gases as a function of ak_F. The full and dashed curves give the LOCV results for $\cosh(\mu r_0=12)$ and δ-function potentials, and the circles show the essentially exact results for the cosh potential obtained with the GFMC method described in Sec. III. The dotted and dash-dotted curves correspond to the conventional BCS results with cosh and δ-function potentials, respectively.

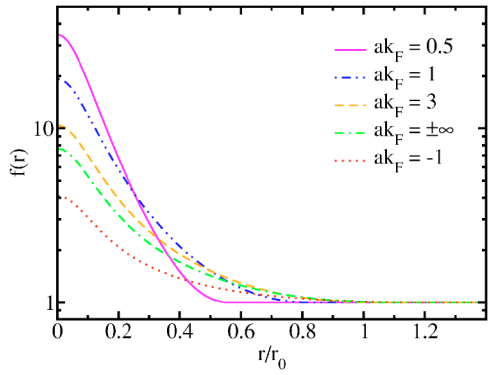

FIG. 2. Correlation function $f(r)$ for different values of ak_F in the LOCV approximation using the cosh potential with $\mu r_0=12$.

becomes close to the molecular binding energy E_{mol} such that $E_{\mathrm{LOCV}}=E_{\mathrm{FG}}+(E_{\mathrm{mol}}/2)+\delta E$. $E_{\mathrm{mol}}/2$ is the term that predominates in this limit. δE is small ($|\delta E|<E_{\mathrm{FG}}$) and negative so that $E_{\mathrm{LOCV}}>E_{\mathrm{mol}}/2$.

When $a>0$, we can obtain another solution of the LOCV equation with a node at $r<d$. This solution was discussed by Cowell *et al.* [18] for cold Bose gases, and at small values of ak_F it gives results in agreement with the low-density expansion [Eq. (1)]. The first term $[(10/9\pi)ak_F]$ is correctly reproduced by LOCV, but the higher-order terms are approximate. In the limit $a\rightarrow\infty$, we have the condition $kd\ \tan(kd)=-1$ discussed in Ref. 18. The solution with one node is $kd=2.7983$ and it gives $E/N=E_{\mathrm{FG}}+(\lambda/2)=E_{\mathrm{FG}}+(\hbar^2/2m)[(kd)^2/d^2]\approx 3.92E_{\mathrm{FG}}$. Results obtained with the δ-function potential, including this unstable region, are shown in Fig. 3. Those corresponding to the nodeless solution of the LOCV equation are represented by a full line, while the dashed line corresponds to the solution with a node.

The state of the gas having a node in the pair correlation function $f(r)$ is unstable because it has energy $>E_{\mathrm{FG}}$, while that with nodeless $f(r)$ has lower energy $<E_{\mathrm{FG}}$ (see Fig. 3). However, it can have a relatively long lifetime because energy conservation prevents two atoms from making the transition to the lower-energy state. At least three atoms are needed, which hinders the transition at low densities. Most of

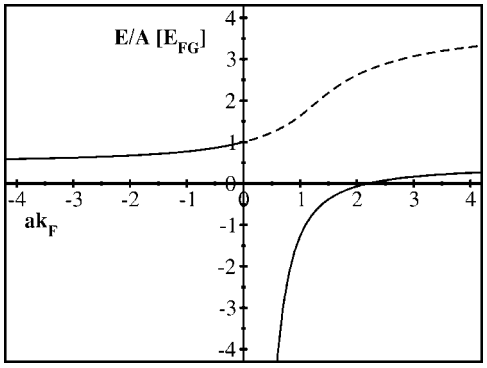

FIG. 3. The LOCV E/A in units of E_{FG} vs ak_F for attractive δ-function potential. The dashed line corresponds to $f(r)$ having one node, and the solid line shows the results with nodeless $f(r)$.

the observed BEC of Bose atoms are in such unstable states in which the $f(r)$ has nodes at small r.

The $E(ak_F)$ shown by the solid line in Fig. 3 corresponds to the stable ground state of the model Hamiltonian with the δ-function interaction. In principle, this state can be exactly calculated by the quantum Monte Carlo method described in the next section. However, when the range of the interaction is finite, as for the cosh model, the system can collapse to a tightly bound state at large density. This instability can be easily seen in the Hartree mean-field approximation in which

$$E_{\mathrm{MF}}(\rho)=E_{\mathrm{FG}}(\rho)+\frac{\rho}{4}I_v,$$

$$I_v=\int v(r)d^3\mathbf{r}, \tag{9}$$

where I_v (<0) is the volume integral of the interaction. At large enough ρ, the interaction energy becomes larger than E_{FG} leading to a tightly bound state.

Consider, for example, a simple square-well potential of range R such that $v(r<R)=-V_0$ and $v(r>R)=0$. Let this potential correspond to $a=\infty$. This means $V_0=\hbar^2\pi^2/4mR^2$ and $I_v=-(4\pi/3)V_0R^3=-(\hbar^2\pi^3/3m)R$. Then

$$E_{\mathrm{MF}}(k_F)=\frac{3}{5}\frac{\hbar^2k_F^2}{2m}\left[1-\frac{5\pi}{54}Rk_F\right]. \tag{10}$$

The collapse occurs at values of $k_F>(54/5\pi)(1/R)$, and can be pushed to higher densities by reducing R, or equivalently increasing μ in the case of the cosh potential. In the present studies, we ignore this collapsed state; assuming that it occurs at too large a density to influence the dilute gas properties.

III. GREEN'S-FUNCTION MONTE CARLO CALCULATIONS

The Green's-function Monte Carlo (GFMC) [20] method is a powerful one for calculating the ground-state properties of many-body quantum systems. It can be used to calculate the ground-state properties of Bose systems with controllable statistical errors without approximation. For the fermion systems, however, we have to deal with the sign problem posed by the antisymmetry of the wave function as discussed below. We begin with a brief overview of the GFMC method.

Let Ψ_i be the eigenstates of $\mathcal{H}$ with eigenvalues E_i. The trial variational wave function Ψ_V, which provides an approximation to the ground state Ψ_0, can be expanded as

$$\Psi_V=\sum_i \alpha_i\Psi_i. \tag{11}$$

In GFMC we project out Ψ_0 from Ψ_V by evolution in imaginary time,

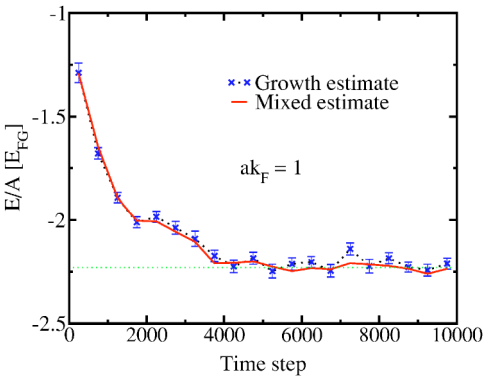

FIG. 4. Mixed and growth estimates of the GFMC energy. The $\tau\to\infty$ asymptotic value is reached after ~5000 time steps. Each time step $\Delta\tau$ is 1.2 $10^{-3}\hbar/E_{\mathrm{FG}}$.

$$\Psi(\tau\to\infty)=\lim_{\tau\to\infty}e^{-(\mathcal{H}-E_T)\tau}\Psi_V$$
$$=\lim_{\tau\to\infty}\sum_i \alpha_i e^{-(E_i-E_T)\tau}\Psi_i\to\alpha_0 e^{-(E_0-E_T)\tau}\Psi_0, \tag{12}$$

where we have shifted the origin of energy to $E_T\approx E_0$ to control the norm of $\Psi(\tau\to\infty)$. In practice, the time evolution is carried out in n small steps,

$$e^{-(\mathcal{H}-E_T)\tau}=\prod e^{-(\mathcal{H}-E_T)\Delta\tau},\quad \Delta\tau=\tau/n, \tag{13}$$

and E_T is tuned to keep $\langle\Psi(\tau)|\Psi(\tau)\rangle$ constant. The tuned E_T provides the growth estimate of the true E_0. An alternative method for calculating the ground-state energy, often with smaller statistical error, is given by the mixed estimate (see Fig. 4)

$$\langle\mathcal{H}\rangle_{\mathrm{mix}}=\frac{\langle\Psi_V|\mathcal{H}|\Psi(\tau\to\infty)\rangle}{\langle\Psi_V|\Psi(\tau\to\infty)\rangle}=E_0\frac{\langle\Psi_V|\Psi(\tau\to\infty)\rangle}{\langle\Psi_V|\Psi(\tau\to\infty)\rangle}=E_0. \tag{14}$$

In general, the time evolution operator or propagator is not known for an arbitrary large value of τ except for a few simple systems. However, we can obtain a small time propagator with controllable errors for any Hamiltonian with static potentials that depend only on the positions of the particles denoted by a $3N$-dimensional configuration vector $\mathbf{R}=\{\mathbf{r}_1,\mathbf{r}_2,\ldots;\mathbf{r}_1',\mathbf{r}_2',\ldots\}$. This is the motivation to write the time evolution as a product of many short time operators [Eq. (13)]. We define the Green's function

$$G(\mathbf{R},\mathbf{R}')=\langle\mathbf{R}|e^{-(\mathcal{H}-E_T)\Delta\tau}|\mathbf{R}'\rangle. \tag{15}$$

The propagation equation becomes

$$\Psi(\mathbf{R},\tau+\Delta\tau)=\int d\mathbf{R}'G(\mathbf{R},\mathbf{R}')\Psi(\mathbf{R}',\tau). \tag{16}$$

The primitive approximation to this Green's function is

$$G(\mathbf{R},\mathbf{R}')\approx e^{-[V(\mathbf{R})-E_T]\Delta\tau/2}G_0(\mathbf{R},\mathbf{R}')e^{-[V(\mathbf{R}')-E_T]\Delta\tau/2}, \tag{17}$$

where $V(\mathbf{R})=\Sigma_{i,j'}v(r_{ij'})$ and $G_0(\mathbf{R},\mathbf{R}')$ is the Green's function for A free particles,

$$G_0(\mathbf{R},\mathbf{R}')=\left[\frac{m}{2\pi\hbar^2\Delta\tau}\right]^{(3/2)A}e^{[-m(\mathbf{R}-\mathbf{R}')^2/2\hbar^2\Delta\tau]}. \tag{18}$$

This approximation has errors of order $\Delta\tau^3$. The total error after n time steps is of the order $\sim n\Delta\tau^3=\tau^3/n^2$. The corrections to this expression can be sampled to make an exact algorithm. Here we use the more common method and make this error as small as we want, by increasing the number of steps n. In practice, this error is made smaller than the statistical sampling errors of the Monte Carlo integration.

A naive quantum Monte Carlo algorithm could start with N_s configuration vectors $\mathbf{R}_i$ sampled from $|\Psi_V|$. These provide the approximate representation

$$\Psi_V(\mathbf{R})\simeq\sum_{i=1}^{N_s}w_i\delta(\mathbf{R}-\mathbf{R}_i), \tag{19}$$

where $w_i=1$ or -1 depending on the sign of Ψ_V. The accuracy of this representation increases with the number of samples N_s. Inserting Eq. (19) into Eq. (16) and using the short-time approximation gives $\Psi(\mathbf{R},\Delta\tau)$ as a sum of normalized Gaussians times weight factors containing the product of the original w_i and the exponentials in the short-time Green's function [Eq. (17)]. Sampling a position from each of the N_s Gaussians gives a representation of $\Psi(\mathbf{R},\Delta\tau)$ as a sum of δ functions times weight factors with signs. This process is repeated n times to obtain $\Psi(\mathbf{R},\tau=n\Delta\tau)$. During the evolution, large magnitude weight factors are converted into multiple copies while small factors are sampled and kept with unit magnitude new weight with a probability proportional to the magnitude of the old weight. The random walk of the weighted δ-function samples representing the propagation of $\Psi(\mathbf{R},\tau)$ therefore consists of diffusing and branching and the number of samples at each time step can vary.

This algorithm suffers from the fermion sign problem. For N_s samples $\mathbf{R}_i$, $1\leqslant i\leqslant N_s$, and weights w_i, the denominator of a matrix element such as the mixed energy will be the sum $\Sigma_{i=1}^{N_s}w_i\Psi_V(\mathbf{R}_i)$. Each w_i carries the sign of the initial sample from Ψ_V, and if the path of the sample i has crossed nodes of Ψ_V an odd number of times, the contribution to the sum will be negative. For large times the contribution of these negative paths almost completely cancel the contribution of positive paths that have not crossed nodes or crossed an even number of times. The signal dies out exponentially compared to the statistical noise. The numerator suffers from the same problem.

The fixed-node [21] approximation deals with the fermion sign problem by restricting the path so that crossings of the nodal surface are not allowed. When this constraint is imposed with the nodal surface of the exact fermion ground state, $\Psi(\mathbf{R},\tau)$ converges to that state. Imposing the nodal surface from an antisymmetric trial function gives an upper bound

$$\lim_{\tau\to\infty}\langle\mathcal{H}\rangle_{\mathrm{mix},\tau}\geqslant E_0. \tag{20}$$

We impose the fixed-node constraint with the nodes of our trial function $\Psi_V(\mathbf{R})$.

Importance sampling is used to control the fluctuations of the weights. The propagation equation is modified by multiplying by a positive importance function. Since we are using the fixed-node approximation, the paths have zero probability of crossing the nodes, and we can take the importance function to be the absolute value of Ψ_V. The propagation equation now becomes

$$[|\Psi_V(\mathbf{R})|\Psi(\mathbf{R},\tau+\Delta\tau)]=\int d\mathbf{R}'\frac{|\Psi_V(\mathbf{R})|}{|\Psi_V(\mathbf{R}')|}G(\mathbf{R},\mathbf{R}')\times[|\Psi_V(\mathbf{R}')|\Psi(\mathbf{R}',\tau)]. \tag{21}$$

The short-time approximation for the importance sampled Green's function is

$$\frac{|\Psi_V(\mathbf{R})|}{|\Psi_V(\mathbf{R}')|}G(\mathbf{R},\mathbf{R}')=G_0\left(\mathbf{R},\mathbf{R}'+\frac{\hbar^2\Delta\tau}{2m}\nabla\ln|\Psi_V(\mathbf{R})|^2\right)\left\{\frac{|\Psi_V(\mathbf{R})|G(\mathbf{R},\mathbf{R}')}{|\Psi_V(\mathbf{R}')|G_0\left(\mathbf{R},\mathbf{R}'+\frac{\hbar^2\Delta\tau}{2m}\nabla\ln|\Psi_V(\mathbf{R})|^2\right)}\right\}$$
$$\approx G_0\left(\mathbf{R},\mathbf{R}'+\frac{\hbar^2\Delta\tau}{2m}\nabla\ln|\Psi_V(\mathbf{R})|^2\right)\left\{e^{-\{1/2[E_L(\mathbf{R})+E_L(\mathbf{R}')]-E_T\}\Delta\tau}\right\}, \tag{22}$$

where the local energy is

$$E_L(\mathbf{R})=\frac{\mathcal{H}\Psi_V(\mathbf{R})}{\Psi_V(\mathbf{R})}. \tag{23}$$

Since G_0 is still a normalized Gaussian, the only changes to the naive algorithm are the sampling of the drifted Gaussian, and the new weight given by the terms in the curly brackets. Notice that if Ψ_V is close to the ground state of $\mathcal{H}$, $E_L(\mathbf{R})$ will have fewer fluctuations than $V(\mathbf{R})$, and the branching of the walk is much reduced. Any paths that cross a node due to the short-time approximation are eliminated.

For N_s samples $\mathbf{R}_i$, all with weight $w_i=1$, at time τ, the mixed energy becomes the average of the local energy

$$\langle\mathcal{H}\rangle_{\mathrm{mix}}=\frac{\sum_{i=1}^{N_s}E_L(\mathbf{R}_i)}{N_s}. \tag{24}$$

Since the fixed-node calculations give an upper bound to the ground-state energy, our strategy (see Ref. [16]) is to choose a trial wave function with variable nodal surfaces and minimize the fixed-node GFMC $\langle H\rangle_{\mathrm{mix}}$.

The trial wave function $\Psi_V(\mathbf{R})$ is now used in three different contexts: (i) as the initial guess of the ground state, (ii) as the importance function in Eq. (21), and (iii) as the node restriction function. The nodes of the Jastrow-Slater wave function [Eq. (4)] equal those of noninteracting Fermi gas and cannot be varied. So that wave function is not useful for the present studies.

From physical considerations, a better trial wave function must reflect the fact that the fermions with attractive interaction can form bound Cooper pairs in the ground state. And from mathematical considerations, the trial wave function must have a variable nodal surface, which can be varied to minimize the fixed-node GFMC energy. The BCS wave function is such a wave function. Commonly, we write

$$|\mathrm{BCS}\rangle_\theta=\prod_p(u_{\mathbf{k}_p}+e^{i\theta}v_{\mathbf{k}_p}\hat{a}^\dagger_{\mathbf{k}_p\uparrow}\hat{a}^\dagger_{-\mathbf{k}_p\downarrow})|0\rangle,$$
$$u^2_{\mathbf{k}_p}+v^2_{\mathbf{k}_p}=1, \tag{25}$$

where $|0\rangle$ denotes the vacuum and $u_{\mathbf{k}_p}$ and $v_{\mathbf{k}_p}$ are real positive numbers. However, this wave function does not correspond to a definite number of particles. In fact, expanding the wave function we can write

$$|\mathrm{BCS}\rangle_\theta=|0\rangle+e^{i\theta}\hat{P}^\dagger|0\rangle+e^{i2\theta}(\hat{P}^\dagger)^2|0\rangle+e^{i3\theta}(\hat{P}^\dagger)^3|0\rangle+\cdots, \tag{26}$$

where $\hat{P}^\dagger=\Sigma_p(v_{\mathbf{k}_p}/u_{\mathbf{k}_p})\hat{a}^\dagger_{\mathbf{k}_p\uparrow}\hat{a}^\dagger_{-\mathbf{k}_p\downarrow}$ is the pair creation operator. The component that corresponds to A particles or $M=A/2$ pairs can be obtained by transforming

$$|\mathrm{BCS}\rangle_A=\frac{1}{2\pi}\int_0^{2\pi}e^{-i\theta M}|\mathrm{BCS}\rangle_\theta d\theta,$$
$$=(\hat{P}^\dagger)^M|0\rangle. \tag{27}$$

This component can be written as an antisymmetrized product of the pair wave functions $\phi(r_{ij'})$,

$$\Psi_{\mathrm{BCS}}(\mathbf{R})=\mathcal{A}[\phi(r_{11'})\phi(r_{22'})\cdots\phi(r_{MM'})],$$
$$\phi(r)=\sum_p\frac{v_{\mathbf{k}_p}}{u_{\mathbf{k}_p}}e^{i\mathbf{k}_p\cdot\mathbf{r}}=\sum_p\alpha_p e^{i\mathbf{k}_p\cdot\mathbf{r}}, \tag{28}$$

where the number of up-spin particles (M) is equal to the number of down-spin particles (M'). The variational parameters α_p are real positive numbers. The free fermion gas, Slater wave function is just a particular case of this wave

function when $\alpha_p \neq 0$ for $|\mathbf{k}_p| \leq k_F$ and $=0$ for $|\mathbf{k}_p| > k_F$.

We also consider systems having unpaired particles. In particular, we can have M pairs and one unpaired up- or down-spin particle. This generalization is necessary as the gap energy Δ is calculated from the odd-even staggering of the ground state energy [16]. With one unpaired ($\uparrow$ or $\downarrow$ spin) particle in the state $\psi_{\mathbf{k}_u}(\mathbf{r})$, with momentum $\mathbf{k}_u$, the trial wave function is given by [22]

$$\Psi_{\mathrm{BCS}}(\mathbf{R}) = \mathcal{A}\{[\phi(r_{11'}) \cdots \phi(r_{MM'})]\psi_{\mathbf{k}_u}(\mathbf{r})\}. \tag{29}$$

The ground state is expected to have $|\mathbf{k}_u| \approx |\mathbf{k}_F|$ in the weakly interacting regime and $\mathbf{k}_u \to 0$ in the strongly interacting regime. This wave function can be calculated as a determinant [22,16], which makes the numerical calculations relatively simple.

Quantum Monte Carlo calculations use a finite number of particles in a cubic periodic box of volume L^3 to simulate the infinite uniform system. The momentum vectors in this box are discrete,

$$\mathbf{k}_p = \frac{2\pi}{L}(n_{px}\hat{x} + n_{py}\hat{y} + n_{pz}\hat{z}), \tag{30}$$

and the system has a shell structure with closures occurring when the total number of particles $=2, 14, 38, 54, \ldots$ for spin-1/2 fermions. The shell number I is defined such that $I = n_x^2 + n_y^2 + n_z^2$, and $E_I = (\hbar^2/2m)(4\pi^2/L^2)I$.

In the present calculations, the pair wave function $\phi(\mathbf{r})$ has the assumed form

$$\phi(\mathbf{r}) = \tilde{\beta}(r) + \sum_{p, I \leq I_C} \alpha_I e^{i\mathbf{k}_p \cdot \mathbf{r}},$$

$$\tilde{\beta}(r) = \beta(r) + \beta(L - r) - 2\beta(L/2) \quad \text{for} \quad r \leq L/2,$$

$$= 0 \quad \text{for} \quad r > L/2,$$

$$\beta(r) = [1 + \gamma br][1 - e^{-cbr}]\frac{e^{-br}}{cbr}. \tag{31}$$

Here $I_c = 4$ is a cutoff shell number. We assume that the contributions of shells with $I > I_c$ to the pair wave function can be approximated by a spherically symmetric function $\tilde{\beta}(r)$ of range $L/2$. We further reduce the statistical fluctuations by using the Jastrow factor along with Ψ_{BCS} in the variational wave function,

$$\Psi_V(\mathbf{R}) = \prod_{i,j'} f(r_{ij'})\Psi_{\mathrm{BCS}}(\mathbf{R}). \tag{32}$$

The Jastrow factor does not change the nodal structure. Thus, the average value of the estimated energy is independent of $f(r)$, but the statistical error is reduced by using the $f(r)$ from LOCV calculations.

It is convenient to require that $\partial\tilde{\beta}/\partial r = 0$ at $r = 0$. This is because the local energy has terms like $(1/r)(\partial\tilde{\beta}/\partial r)$, which can have large fluctuations at the origin when $\partial\tilde{\beta}/\partial r \neq 0$ at $r = 0$. The factor $[1 - e^{-cbr}]$ cuts off $1/cbr$ dependence of β at $br < 1/c$. The energies are not too sensitive to the parameter c, and its value is fixed at 10. In addition, γ is chosen such that $\partial\tilde{\beta}/\partial r = 0$ at $r = 0$; its value is 6 in the limit $L \to \infty$.

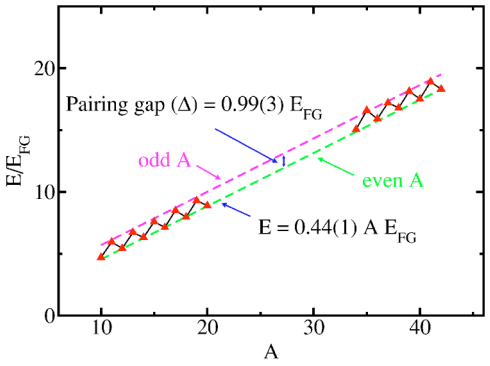

FIG. 5. $E(A)$ when $ak_F = -\infty$ from Ref. 16.

The variational parameters are $\{\alpha_0, \alpha_1, \ldots, \alpha_{I_c}\}$ and b. We wish to find a set of these parameters that minimize the fixed-node GFMC estimate of energy. However, considering that we have to allow simultaneous variation of all the parameters, methods based on unguided variation become difficult, if not infeasible. Again, we rely on the GFMC procedure itself to optimize these parameters. Initial configurations are obtained with a random distribution of the parameters centered around a reasonable guess. Each of them is propagated according to the nodal constraints provided by their parameters with a single E_T. The paths with the smallest $\langle \mathcal{H} \rangle_{\mathrm{mix}}$ acquire large amplitudes or weights as $\tau \to \infty$. The average among these paths gives an optimization over the initial random distribution. This process is repeated several times until convergence is achieved.

When we have an odd number of particles, the ground-state momentum $\mathbf{k}_u$ [Eq. (29)] is an additional variational parameter. We minimize the fixed-node GFMC energy of systems with odd A by varying $\mathbf{k}_u$. As discussed in the next section, the magnitude of $\mathbf{k}_u$ changes from k_F to 0 as the interaction strength increases and we go from the weakly interacting BCS to the strongly interacting BEC regime. The gap energy is obtained from the odd-even staggering of the total energy

$$\Delta(2M + 1) = E(2M + 1) - \frac{1}{2}[E(2M) + E(2M + 2)]. \tag{33}$$

In doing so, the effects of interaction among quasiparticles are neglected.

Results for $ak_F = \infty$ are shown in Fig. 5. The energy per particle E/A and the gap Δ do not have a significant A dependence in this case. These results were reported in Ref. 16, and results for other values of ak_F are presented in the next section.

IV. RESULTS

The values of the parameters, α_{0-4} and b, of the BCS wave function are to be determined by minimizing the fixed-node GFMC mixed energy for each value of ak_F and A. The

TABLE I. Optimum values of the variational parameters.

ak_F	A	α_0	α_1	α_2	α_3	α_4	b
−1	10	1.00	0.05	0	0	0	NA
	14	1.00	1.00	0.010	0	0	NA
	20	1.00	1.00	0.104	0.024	0	NA
−3	10	0.40	0.165	0.019	0.009	0.002	1.13
	14	0.28	0.280	0.020	0.006	0.003	1.05
−10	10	0.295	0.096	0 018	0.007	0.002	0.48
	14	0.220	0.130	0.019	0.007	0.003	0.44
∞	10	0.315	0.103	0.020	0.010	0.003	0.50
	14	0.181	0.102	0.024	0.006	0.004	0.44

minimum energy obtained is our estimate for the ground-state energy of the system. The values of the parameters that minimize this energy are not very sensitive to A, the number of particles in the box. We find it sufficient to determine the optimum parameters at $A=10$, 14, and 20, and interpolate their values in the $A=10$, 14 and $A=14$, 20 ranges. The values of the parameters at these values of A are listed in Table I.

At $ak_F=-1$, the lowest energies are obtained without any short range $\tilde{\beta}(r)$ and the optimum pair function has contributions only from the states with $I\leqslant 3$. This is consistant with the weak-coupling BCS theory in which α_k goes to zero when $k-k_F$ becomes large.

When $1/ak_F>-1$, lower energies are obtained with $\tilde{\beta}(r)\neq 0$. In most cases, the values of the parameters do not change significantly between $A=14$ and 20 The values listed in Table I for $A=14$ are used for $14\leqslant A\leqslant 20$.

In the $0<1/ak_F\leqslant 2$ range, the optimum values of the parameters of Ψ_{BCS} do not seem to change significantly with the ak_F. We have not obtained any significant improvements to the energy from varying the parameters in the region $1/ak_F>0$. In this region, we retain the values found for $1/ak_F=0$ and $A=14$. Recall that only the nodal surfaces of the ground-state wave function are constrained by those of Ψ_{BCS}. The complete Ψ_V has an additional product of Jastrow pair correlation functions $f(r_{ij'})$ which depends on ak_F, and

TABLE II. Values of k_u^2 in units of $(2\pi/L)^2$.

ak_F	$A=11,13$	$A=15,17,19$
0	1	2
−1	1	2
−3	1	2
−10	1	1
∞	1	1
10	1	1
3	1	1
2	0 or 1	0 or 1
1	0	0
0.75	0	0
0.5	0	0

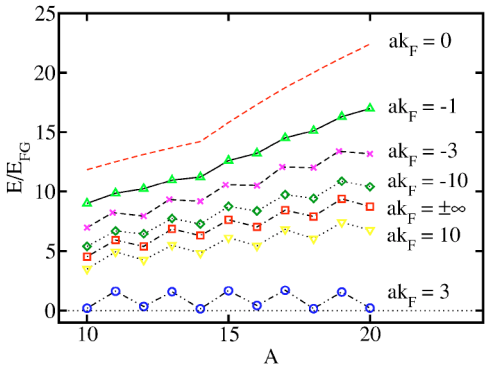

FIG. 6. $E(A)$ for $1/ak_F\leqslant 1/3$.

the true ground-state wave function changes continuously with ak_F.

The magnitude of the momentum $\mathbf{k}_u$ of the unpaired particle in the ground state is also determined by minimizing the GFMC fixed-node energy. The minimum values are listed in Table II. In the weak-coupling limit, the BCS ground state for odd A has $|\mathbf{k}_u|=|\mathbf{k}_F|$. In the periodic box, the value of k_F^2 is 1 for $2<A\leqslant 14$, and 2 for $14<A\leqslant 38$ in units of $(2\pi/L)^2$. In the $ak_F=0$ to −3 range, the minimum values of k_u^2 are as indicated by the weak-coupling BCS theory. However, in the −10 to 3 range, the k_u^2 is 1 for the entire range (11 to 19) of odd values of A considered. At $ak_F=2$, the states with $k_u^2=0$ and 1 are almost degenerate, and for $1/ak_F>0.5$, the ground states of odd A systems have $\mathbf{k}_u=0$, as expected when the system consists of bound molecules condensed in the zero momentum state, and the unpaired particle also in the $\mathbf{k}_u=0$ state.

The calculated values of the ground-state energy are shown in Figs. 6 and 7. The systems with $1/ak_F\leqslant 1/3$ seem to have $E>0$, while those with $1/ak_F>1/3$ can have $E<0$. When $1/a>0$, the two-body interaction is strong enough to bind two particles and form molecules with energy E_{mol}. The energy per particle, E/A, of the superfluid Fermi gas is compared with $E_{\mathrm{mol}}/2$ in Fig. 8. Within the computational errors $E/A>E_{\mathrm{mol}}/2$ (see Table III), however at $1/ak_F\geqslant 0.5$ we find that E/A is very close to $E_{\mathrm{mol}}/2$. This behavior also indicates that at these values of ak_F the system approaches that composed of Bose molecules forming a BEC. It has been argued that the interaction between these molecules is weakly repul-

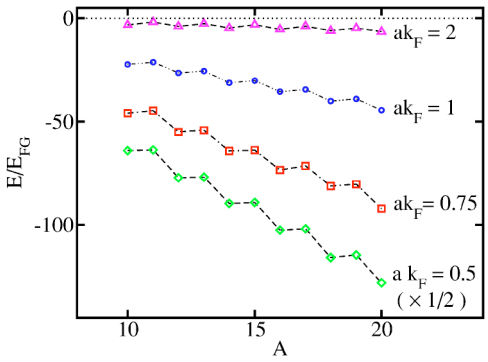

FIG. 7. $E(A)$ for $1/ak_F>1/3$. The results for $ak_F=0.5$ have been multiplied by 0.5 for graphing.

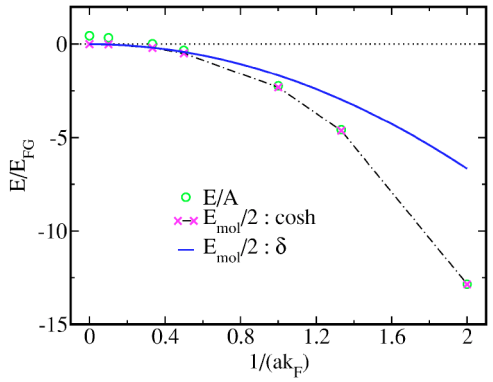

FIG. 8. E/A and $E_{\mathrm{mol}}/2$ for positive values of $1/ak_F$ for the cosh ($\mu r_0=12$) potential and $E_{\mathrm{mol}}/2$ for the δ-function potential.

sive, with a molecule-molecule scattering length given by $a_{\mathrm{mm}}=0.6a$ [23]. In this case, the E/A will always be greater than $E_{\mathrm{mol}}/2$, and the gas will have positive pressure, E/A increasing with the gas density or k_F.

The pairing gaps calculated from the odd-even energy difference [Eq. (33)] are shown in Figs. 9 and 10. These gaps are not very sensitive to A, and they are compared with the predictions of BCS [3] and Gorkov [5] estimates given by

$$\Delta_{\mathrm{BCS}}=\frac{8}{e^2}T_F\, e^{\pi/(2ak_F)},$$

$$\Delta_{\mathrm{Gorkov}}=\left(\frac{2}{e}\right)^{7/3}T_F\, e^{\pi/(2ak_F)}=\frac{1}{2}\left(\frac{2}{e}\right)^{1/3}\Delta_{\mathrm{BCS}}, \qquad (34)$$

where the chemical potential is approximated by T_F as when $1/ak_F\ll 0$. At $1/ak_F\ll 0$, the calculated gaps are in between these estimates, while at positive values of $1/ak_F$ they approach $-E_{\mathrm{mol}}/2$ as expected for a gas of Bose molecules (see Fig. 10 and Table III).

Figures 8 and 11 also show the E_{mol} for a δ-function interaction in addition to those for the present cosh potential with $\mu r_o=12$. The two potentials give essentially the same results for $1/ak_F<0.5$, but at larger values the cosh potential is more attractive. The values of the rms radius R_{rms} of the molecule are listed in Table III. At large values of $1/ak_F$, the

TABLE III. Summary of the results in the strongly interacting regime.

$1/ak_F$	Δ/E_{FG}	$E_{\mathrm{GFMC}}/AE_{\mathrm{FG}}$	$E_{\mathrm{mol}}/2E_{\mathrm{FG}}$	R_{rms}/r_0	μR_{rms}
0	0.99(4)	0.44(1)	0	∞	∞
0.1	1.03(5)	0.34(1)	−0.01(1)	3.69	44.3
$0.\dot{3}$	1.37(5)	0.02(1)	−0.20(1)	1.21	14.5
0.5	1.80(5)	−0.33(1)	−0.49(1)	0.74	8.9
1.0	3.2(1)	−2.23(1)	−2.31(1)	0.38	4.6
$1.\dot{3}$	5.7(3)	−4.58(2)	−4.63(1)	0.28	3.4
2.0	14.0(5)	−12.84(3)	−12.86(1)	0.19	2.3

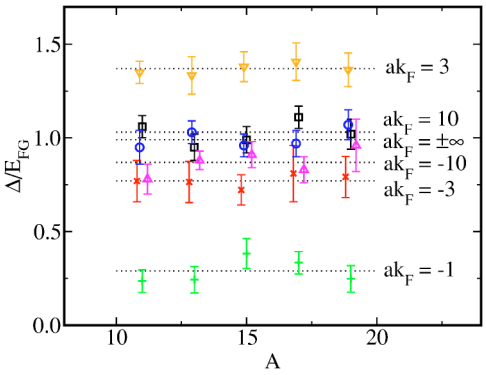

FIG. 9. $\Delta(A)$ for $1/ak_F\leqslant 1/3$.

μR_{rms} is not very large for the present choice of $\mu r_0=12$, and much larger values of μ should be used to approximate the δ-function interaction.

The pressure ($P=\rho^2[\partial(E/A)/\partial\rho]$) and the adiabatic index [$\Gamma=(\rho/P)(\partial P/\partial\rho)$] of the superfluid gas in the range $-20<ak_F<0$ are shown in Fig. 12. For noninteracting Fermi gas ($ak_F=0$), $E/A=E_{\mathrm{FG}}$ and we have $P=(2/3)\rho E_{\mathrm{FG}}$ and $\Gamma=5/3$. In the limit $ak_F\to 0$, we can use the low-density expansion [Eq. (1)] to obtain

$$P(ak_F\to 0)\approx\frac{2}{3}\rho E_{\mathrm{FG}}\left(1+\frac{5}{3\pi}ak_F\right),$$

$$\Gamma(ak_F\to 0)\approx\frac{5}{3}+\frac{5}{9\pi}ak_F. \qquad (35)$$

In the $ak_F\to-\infty$ limit, we have $E/A=\xi E_{\mathrm{FG}}$, therefore

$$P(ak_F\to-\infty)=\frac{2}{3}\xi\rho E_{\mathrm{FG}},$$

$$\Gamma(ak_F\to-\infty)=\frac{5}{3}, \qquad (36)$$

where $\xi=0.44\pm0.01$ according to the present calculations.

The calculated value of $P(ak_F)/(\rho E_{\mathrm{FG}})$ is $2/3$ at $ak_F=0$ and decreases monotonically to $(2/3)\xi$ as $ak_F\to-\infty$. However, the adiabatic index $\Gamma(ak_F)$ is $5/3$ for both $ak_F=0$ and $ak_F=-\infty$, and has a minimum value of ~ 1.6 at $ak_F\sim-1.3$.

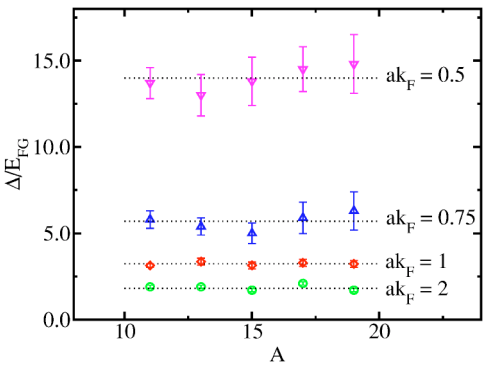

FIG. 10. $\Delta(A)$ for $1/ak_F>1/3$.

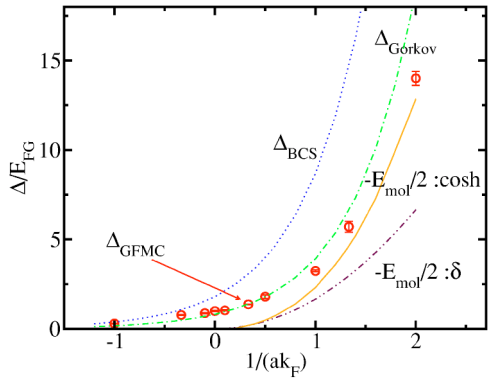

FIG. 11. Calculated values of $\Delta_{\mathrm{GFMC}}(ak_F)$ (cosh, $\mu r_0=12$ potential) are compared with various estimates of $\Delta(ak_F)$ and $-E_{\mathrm{mol}}/2$. The BCS and Gorkov estimates do not depend on the shape of the potential, while $-E_{\mathrm{mol}}/2$ is shown for both cosh (solid line) and δ-function (dash double dot) potentials. Δ_{BCS} and Δ_{Gorkov} assume the chemical potential $\approx T_F$ throughout the whole range of ak_F [see Eq. (34)].

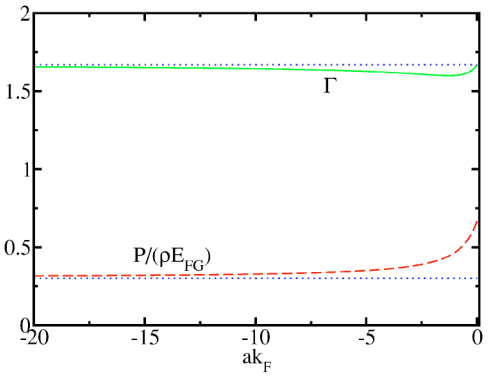

FIG. 12. Pressure (P, dashed curve) and adiabatic index (Γ, continuous curve) in the BCS regime ($ak_F<0$). In the dilute limit ($ak_F\to 0$) we have $P/(\rho E_{\mathrm{FG}})\to 2/3$ and $\Gamma\to 5/3$. In the dense limit ($ak_F\to-\infty$) we have $P/(\rho E_{\mathrm{FG}})\to 0.44(2/3)$ and $\Gamma\to 5/3$. Γ has a minimum at $ak_F\sim -1.3$.

V. CONCLUSIONS

The present work shows that accurate calculations of the pairing gaps and energies of superfluid Fermi gases are possible with the fixed-node GFMC method. The unknown nodal surfaces can be determined variationally by minimizing the fixed-node GFMC energy. This method gives the exact result in the $1/ak_F\to-\infty$ (Fermi gas) and $1/ak_F\to+\infty$ (BEC of molecules) limits for short-range attractive interaction, and seems to overcome the fermion sign problem. An alternative method based on path-integral Monte Carlo simulations is also being developed [24].

Our results are in qualitative agreement with the known BCS-BEC crossover model (see Leggett [3]) where the gap and chemical potential (μ_0) are calculated self-consistently. The gap is determined as the minimum of the Bogoliubov quasiparticle energy $E_{\mathbf{k}}=\sqrt{(\epsilon_{\mathbf{k}}-\mu_0)^2+|\Delta'_{\mathbf{k}}|^2}$, where $\epsilon_{\mathbf{k}}=\hbar^2k^2/2m$ is the single-particle excitation energy and $\Delta'_{\mathbf{k}}$ is the gap parameter. Two limiting cases were considered in this referenced article. For $1/ak_F\to-\infty$, $\mu_0\approx T_F>0$, the minimum of $E_{\mathbf{k}}$ occurs at $k=k_F$ and the minimum quasiparticle energy $\Delta=\Delta'_{k_F}=(8/e^2)T_Fe^{\pi/(2ak_F)}$. However, for $1/ak_F\to+\infty$, $\mu_0\approx E_{\mathrm{mol}}/2<0$, the minimum of $E_{\mathbf{k}}$ is at $k=0$, and its value $\Delta=|\mu_0|\sim|E_{\mathrm{mol}}|/2$ because $\Delta'_{\mathbf{k}}\sim 0$. The BCS-BEC crossover takes place when $\mu_0=0$ and this corresponds to ak_F positive and of the order 1. The odd-even staggering $\Delta(2M+1)$ given by Eq. (33) presumably equals the minimum quasiparticle energy in the limit $M\to\infty$.

According to Leggett's description, in the weak BCS superfluids the ground state of systems with an odd number of particles is expected to have momentum k_F, while in the molecular liquid with BEC it is expected to have zero momentum. With this criterion the calculated values of k_u^2 (Table II) suggest that the BCS-to-BEC transition occurs in the range $-0.5<1/ak_F<0.5$. It appears to be a smooth transition or crossover.

A recent experiment by Bartenstein *et al.* also seems to corroborate some of our findings. In fact, in their paper [25] the BCS-BEC crossover regime for ^{6}Li is reported to be $-0.5\lesssim 1/ak_F\lesssim 0.5$. In addition, in the unitary limit ($ak_F=\pm\infty$) they measured $E/A=0.32^{+13}_{-10}E_{\mathrm{FG}}$, which includes within its range our result $E/A=(0.44\pm0.01)_{\mathrm{FG}}$.

We can notice that in the BCS regime Δ is much smaller than E/A, while in the BEC regime $\Delta\sim|E|/A\sim|E_{\mathrm{mol}}|/2$. However, in the transition region Δ is significantly larger than $|E|/A$.

ACKNOWLEDGMENTS

The work of J.C. is supported by the U.S. Department of Energy under Contract No. W-7405-ENG-36, while that of S.Y.C. and V.R.P is partly supported by U.S. National Science Foundation via Grant No. PHY-00-98353.

[1] L. N. Cooper, R. L. Mills, and A. M. Sessler, Phys. Rev. **114**, 1377 (1959).
[2] C. J. Pethick and D. G. Ravenhall, Annu. Rev. Nucl. Part. Sci. **45**, 429 (1995).
[3] A. J. Leggett, in *Modern Trends in the Theory of Condensed Matter*, edited by A. Pekalski and R. Przystawa (Springer-Verlag, Berlin, 1980).
[4] M. Randeria, in *Bose-Einstein Condensation*, edited by A. Griffin, D. W. Snoke, and S. Stringari (Cambridge University Press, Cambridge, 1995).
[5] L. P. Gorkov and T. K. Melik-Barkhudarov, Sov. Phys. JETP **13**, 1018 (1961).
[6] B. De Marco and D. S. Jin, Science **285**, 1703 (1999).
[7] K. M. O'Hara, S. L. Hemmer, M. E. Gehm, S. R. Granade, and J. E. Thomas, Science **298**, 2179 (2002).
[8] J. Stenger, S. Inouye, M. R. Andrews, H.-J. Miesner, D. M.

Stamper-Kurn, and W. Ketterle, Phys. Rev. Lett. **82**, 2422 (1999).
[9] J. L. Roberts, N. R. Claussen, S. L. Cornish, E. A. Donley, E. A. Cornell, and C. E. Wieman, Phys. Rev. Lett. **86**, 4211 (2001).
[10] C. A. Regal, C. Ticknor, J. L. Bohn, and D. S. Jin, Nature (London) **424**, 47 (2003).
[11] C. A. Regal, M. Greiner, and D. S. Jin, Phys. Rev. Lett. **92**, 040403 (2004).
[12] W. Lenz, Z. Phys. **56**, 778 (1929).
[13] K. Huang and C. N. Yang, Phys. Rev. **105**, 767 (1957).
[14] G. A. Baker, Phys. Rev. C **60**, 054311 (1999).
[15] H. Heiselberg, Phys. Rev. A **63**, 043606 (2001).
[16] J. Carlson, S.-Y. Chang, V. R. Pandharipande, and K. E. Schmidt, Phys. Rev. Lett. **91**, 050401 (2003).
[17] V. R. Pandharipande, and H. A. Bethe, Phys. Rev. C **7**, 1312 (1973).
[18] S. Cowell, H. Heiselberg, I. E. Mazets, J. Morales, V. R. Pandharipande, and C. J. Pethick, Phys. Rev. Lett. **88**, 210403 (2002).
[19] V. R. Pandharipande and K. E. Schmidt, Phys. Rev. A **15**, 2486 (1977).
[20] M. H. Kalos, D. Levesque, and L. Verlet, Phys. Rev. A **9**, 2178 (1974).
[21] J. B. Anderson, J. Chem. Phys. **63**, 1499 (1975).
[22] J. P. Bouchaud, A. Georges, and C. Lhuillier, J. Phys. (Paris) **49**, 553 (1988).
[23] D. S. Petrov, C. Salomon, and G. V. Shlyapnikov, e-print cond-mat/0309010.
[24] J. Shumway and D. M. Ceperley, J. Phys. IV **10**, 3 (2000).
[25] M. Bartenstein, A. Altmeyer, S. Riedl, S. Jochim, C. Chin, J. H. Denschlag, and R. Grimm, Phys. Rev. Lett. **92**, 120401 (2004).